HiSST: 2nd International Conference on
High-Speed Vehicle Science Technology
11 – 15 September 2022, Bruges, Belgium

Sounding Rocket Flight Experiment ATEK
- A Testbed for Technologies and Components of Launcher Stages -

A. Gülhan[1], A. Kallenbach[2], I. Petkov[3], F. Klingenberg[4], F. Siebe[5]

Abstract

The ATEK flight experiment was successfully launched on 13th July 2019 from the launch site Esrange in Kiruna and provided valuable flight data. The second stage and the payload reached an apogee of approx. 240 km and continued the descent without any thrust and landed approx. 500 seconds after the take-off at a distance of approx. 67 km from the launch site. The payload was decelerated in the late subsonic flight phase using a parachute to avoid a hard impact on ground after a 800 seconds flight time. The Health Monitoring System allowed the measurement of aerothermal and mechanical loads on the hybrid payload structure, motor adapter, motor case, tail can and fins along the complete flight. Part of the data has been transmitted during flight to ground via telemetry at a low sampling rate of several Hertz. In addition, several impact-resistant data acquisition units could acquire the data at a high sampling rate of several Kilohertz and stored it onboard. The hybrid payload structure and health monitoring data acquisition units have been recovered after the flight and showed complete functionality.

Keywords: *ATEK, Flight Experiment, Hybrid Module, Health Monitoring, Impact-resistant Design*

1. Introduction

Following previous development work concerning in-flight technology demonstration using sounding rockets, DLR performed in July 2019 the ATEK flight experiment [1,2,3]. The main objective of the ATEK project (Technologies for Launcher Stages and Components) has been the development and flight qualification of structures, measurement techniques and analysis tools, which are used for thermo-mechanical evaluation of launchers. Such flight data, in combination with ground experiment results, are the key element of the validation of physical models, numerical simulation and system analysis tools, which are used to evaluate and to design future space transportation systems. ATEK flight configuration consisted of Health-Monitoring-Systems for critical launcher components and a hybrid payload structure.

The flight experiment has been successfully launched on 13th July 2019 from the launch site Esrange in Kiruna Sweden and reached an apogee of approx. 240 km (**Fig 1**). Approx. 13 seconds after take-off, the first stage S31 of the VSB30 launcher is burned-out and separated. The second stage S30 is ignited immediately afterwards and provided thrust for 29 seconds. Three seconds after a de-spin

[1] *ATEK Project Manager* and *Head of Department, DLR Institute of Aerodynamics and Flow Technology, Supersonic and Hypersonic Technologies Department, Cologne, Germany, ali.guelhan@dlr.de*
[2] *Research Scientist, DLR Institute of Space Operations and Astronaut Training, Mobile Rocket Base (MORABA) Department, Oberpfaffenhofen, Germany*
[3] *Research Scientist, DLR Institute of Structures and Design, Space System Integration Department, Stuttgart, Germany.*
[4] *Research Engineer, DLR Institute of Aerodynamics and Flow Technology, Supersonic and Hypersonic Technologies Department, Cologne, Germany.*
[5] *Research Scientist, DLR Institute of Aerodynamics and Flow Technology, Supersonic and Hypersonic Technologies Department, Cologne, Germany.*

maneuver by a Yo-Yo system the S30 is separated from the payload. During this first 60 seconds an aerodynamically stable flight could be enabled. The second stage and the payload continued the descent without any thrust and landed approx. 500 seconds after the take-off at a distance of approx. 67 km from the launch site. The payload has been decelerated in the late subsonic flight phase using a parachute to avoid a hard impact on ground after 800 seconds flight time. The stage S30 experienced a hard ground impact after a planned uncontrolled descent flight.

Fig 1: ATEK flight configuration launching from the Skylark tower of Esrange

2. Flight Experiment Configuration

ATEK flight experiment contained two different types of payloads on board. The micro-gravity experiments block was a part of the ongoing DLR's research programme concerning micro-g activities (called as MAPHEUS-8). The second group of payloads were devoted to flight qualification of launcher technologies wrt aerothermodynamics, high temperature structures and health monitoring instrumentation. Such scaled sounding rocket experiment in combination with ground tests and numerical rebuilding should allow us to perform a reliable extrapolation of full-scale flight configuration. Therefore, the launcher related topics of the experiment were supported by detailed ground qualification and numerical simulation tasks within the ATEK project. A further very important aspect was the establishment and verification of the sounding rocket based flight test platform for future DLR's high speed flight experiments. The main scientific objectives of the ATEK flight experiment can be summarized as

- Flight qualification of a cork based thermal protection system for hybrid module
- Flight qualification of a new hybrid structure module
- Development of a health monitoring instrumentation system for hybrid module, fins, tailcan and nozzle and its flight qualification
- Development of a modular and impact-resistant data acquisition system with different sampling rates and its flight qualification
- In-flight application of a Fibre Optics Sensing System (FOS) for in-flight measurement of the motor case surface temperature.

The ATEK flight experiment consisted of the first stage motor S31, second stage motor S30, motor adapter, micro-gravity experiments block (MAPHEUS-8), hybrid module and several service / payload support modules (**Fig 2**). The total length of the flight configuration was approx. 12.5 m. The payload section had a diameter of 17" (438 mm).

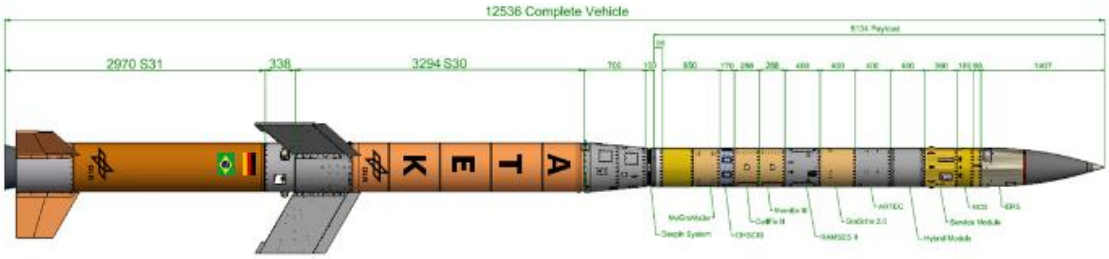

Fig 2: ATEK flight configuration based on VSB-30 rocket

Fig 3 shows critical flight events, which are decisive for a successful flight. Therefore, the flight dynamic behaviour of the vehicle has to be proved at this flight points. Due to the instrumentation and further hardware accommodated in the tailcan, the centre of gravity of the S30 stage moved backwards and caused reduction of the aerodynamic stability margin of this stage. To counteract this effect, a 26 kg balance mass has been integrated into the balance ring between RCS and ERS modules in the forebody area of the MAPHEUS-8 payload. Furthermore, an empty segment has been inserted between the motor adapter and micro-gravity experiment modules.

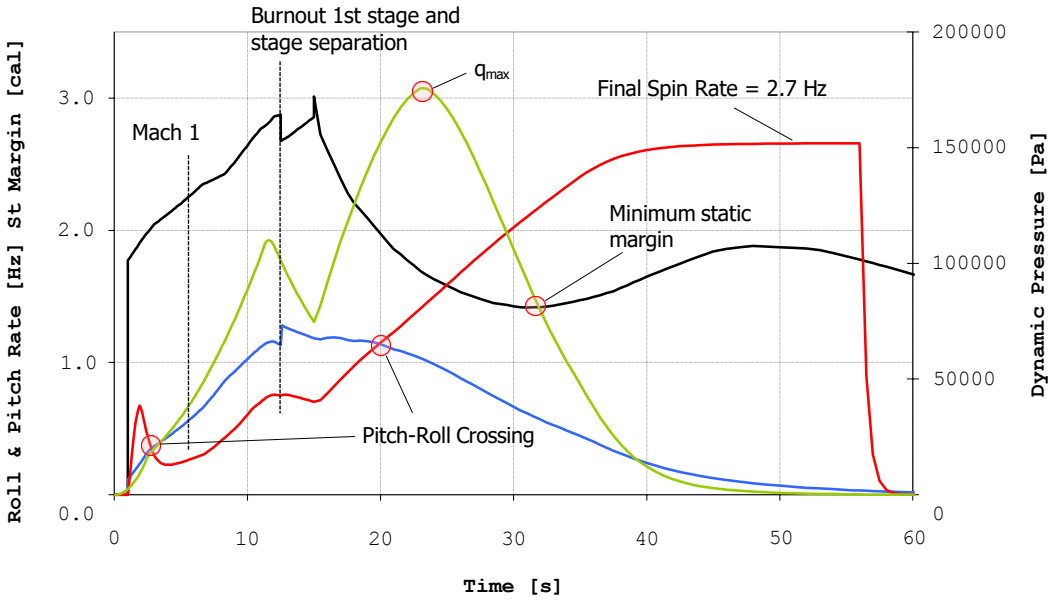

Fig 3: Critical flight events

In order to check the impact of these measures on the static stability, dedicated aerodynamic studies have been carried out using simplified and CFD tools. Fig 4 shows computed roll and natural pitch rates in the ascent flight phase and corresponding static margin data. At the most critical trajectory point regarding flight stability, CFD prediction provides a static margin of 1.05 cal, which uses the motor diameter of 0.557 m as reference.

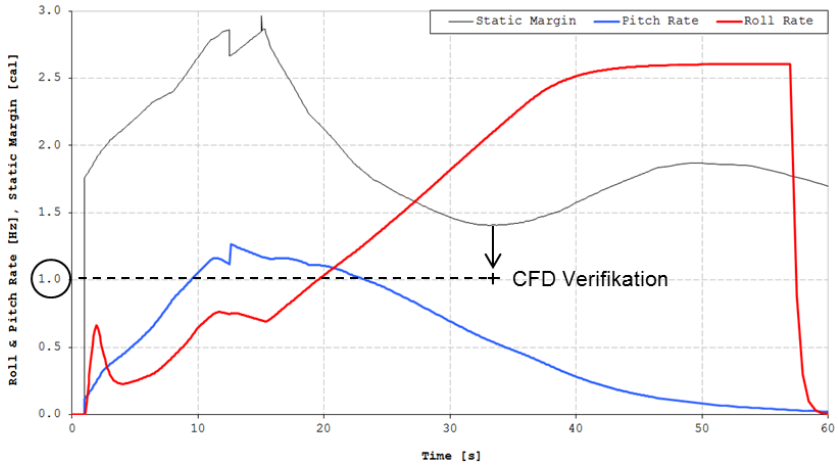

Fig 4: Static stability margin of the second stage S30

Predicted flight trajectory of the S31 booster results in an apogee of 7.9 km, a nominal impact 0.91 km down range and a total flight time of 91 s.

The second stage booster S30 is to be actively separated from the payload 60 seconds after the lift-off and will be exposed to severe conditions of an uncontrolled descent flight and high-speed ground impacts without parachute. The instrumentation of components of this stage like the motor adapter, motor case, tailcan and fins with integrated impact-resistant data acquisition memory units should deliver important data.

To decelerate the payload sufficiently before initiating the parachute sequence, and to grant high deployment reliability, it is a requirement that the payload must finally attain a stable flat spin when falling through the low atmosphere. To ensure this flight condition a certain value for the distance between centre-of-pressure and centre-of-gravity of has to be guaranteed. Fig 5 shows the re-entry configuration of payloads with integrated parachute in the last segment of it.

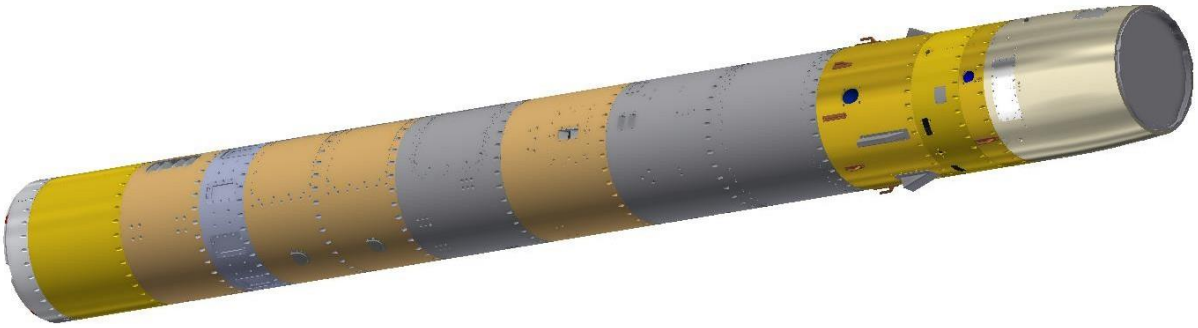

Fig 5: Re-entry flight configuration of payloads

3. Ground Qualification

For sounding rocket flight experiments DLR uses normally metallic structures like Aluminum alloys. For the mass reduction DLR's institute of Structures and Design in Stuttgart developed a new hybrid module made of CFRP and metallic structure (Fig 6). The high application temperature of the CFRP segment during ATEK flight experiment required using high temperature matrix polymers. The difference of thermal conductivities of CFRP block and Aluminum flanges has been compensated by a suitable choice

of fiber orientation during manufacturing. A cork based thermal protection layer was applied for the thermal protection.

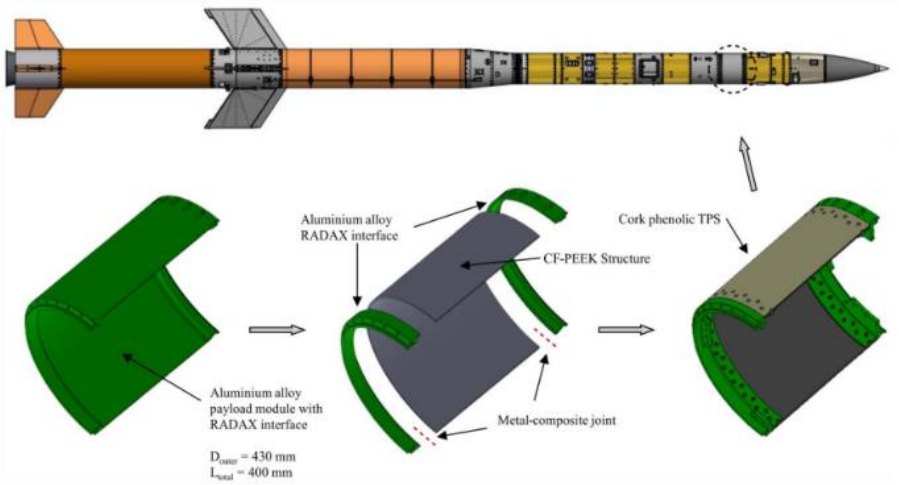

Fig 6: ATEK modules in original and hybrid design format

Mechanical test on the hybrid segment was carried out using a facility with 1000 kN maximum force. As shown in Fig 7 an Aluminium base plate and a Radax interface allowed applying high loads in axial direction. The module also passed bending tests with 18 kNm bending moment and 7.4 kN shear force (Fig 7, right).

Fig 7: Mechanical tests (left) and bending test (right) on hybrid module

Flight preparatory activities included check of mechanical fit, test of mechanical interfaces, air bearing tests, bench tests and environmental tests. The air bearing facility of MORABA allowed testing the functionality of the RCS (Reaction Control System) (Fig 8). During bench test all sub-systems have been tested simultaneously by simulating the flight case. Performing these tests with ten different scientific payloads was a real challenge. Environmental tests have been performed in the laboratory of Airbus in Ottobrunn (Fig 9). During this intense test-week the payloads and tailcan have been balanced in terms of moment of inertia, main properties of the vehicle like mass, moment of inertia and center of gravity have been measured. Finally, vibration tests on the complete payload and tailcan have been performed.

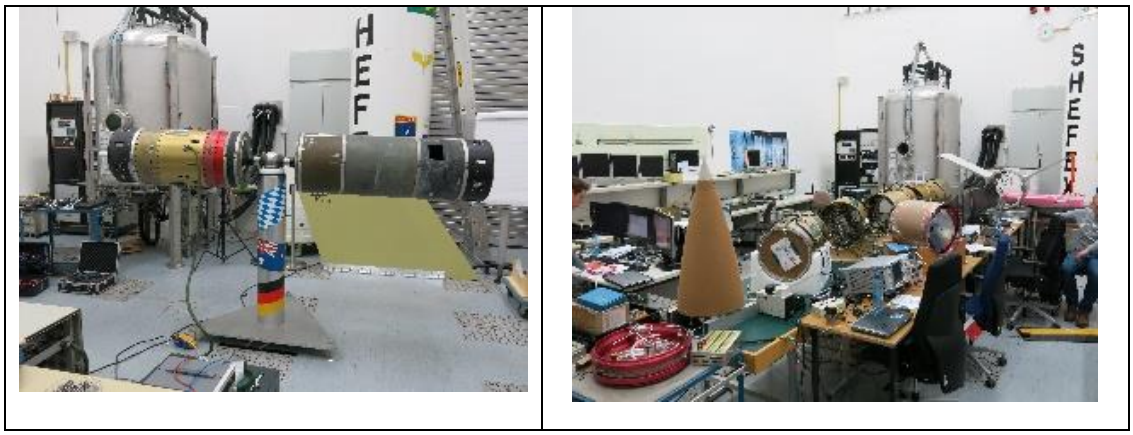

Fig 8: RCS air bearing test (left) and bench test (right) in MORABA laboratory

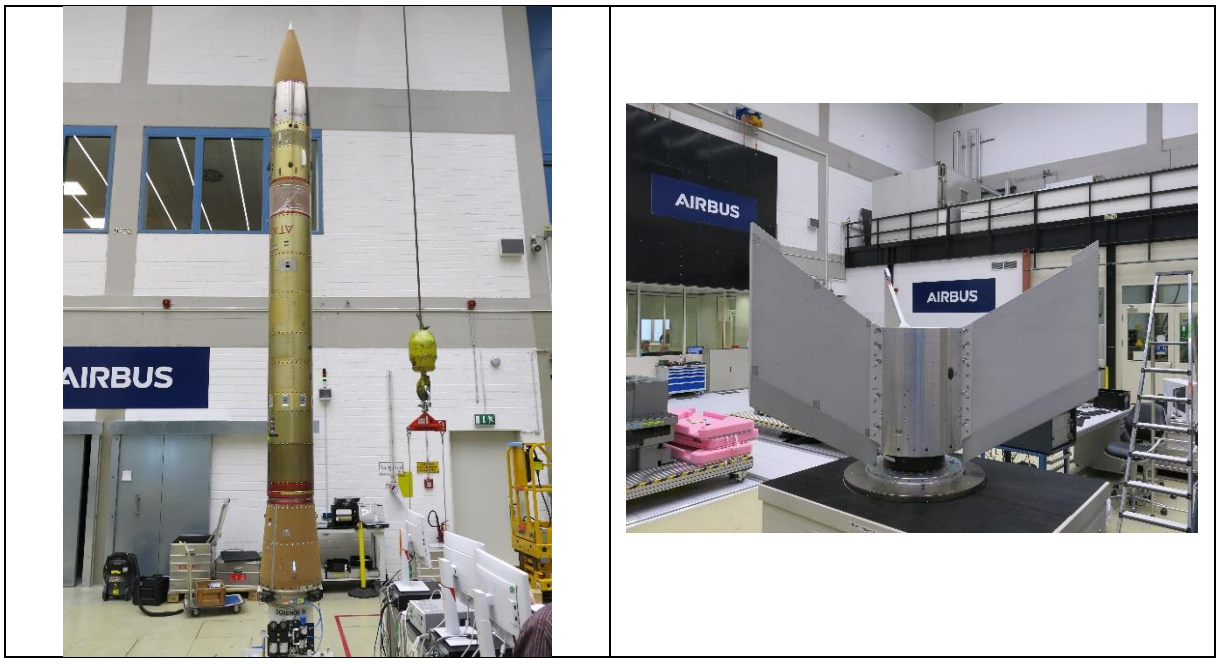

Fig 9: Moment of inertia tests on the ATEK/MAPHEUS-8 payload in Airbus laboratory (left) and Spin balancing of Tailcan assembly (right)

After successful bench and environmental tests, the flight hardware has been transported to Esrange close to Kiruna, Sweden. The complete team arrived in Esrange on 29.05.2019. The instrumentation of the S30 motor using FOS sensors required a lot of effort.

Finally, the complete science payload sections with a diameter of 438 mm reached a total mass of 434 kg, which includes also instrumented payload adapter, instrumented motor adapter with integrated despin ring and instrumented tailcan and fin section. The total take-off mass and the length of the complete flight configuration were 2669 kg and 12536 mm, respectively.

4. Flight Experiment

After successful bench test and flight simulation the ATEK flight configuration has been integrated into the Skylark Tower on 09.06.2019. The successful test countdown and suitable wind conditions allowed launching ATEK flight experiment (Table 1). The flight experiment has been successfully launched on 13th July 2019 from the launch site Esrange in Kiruna Sweden and reached an apogee of approx. 240 km (Fig 1).

Table 1: Reference data of launch preparation

Launch Date and Time	13/06/2019, 02:21 UTC (04:21 LT)
Launch Site	Esrange
Launcher	Skylark Tower
Vehicle	VSB-30
Number of Hot Countdown Days	1
Weather Conditions	Partly cloudy sky
Atmospheric Temperature	+8°C
Atmospheric Pressure	986 hPa
Temperature at Launcher (Payload Level)	+20°C
Ballistic Wind Speed	4.2 m/s
Ballistic Wind Direction	224 deg
Nominal/Final Launcher Elevation	87.8/86.4 deg
Nominal/Final Launcher Azimuth	352/17 deg

The thrust performance of the first stage S31 and second stage S30 was as predicted. This allowed flying the trajectory as planned. Correct spin rate setting led to an ascent flight with a small pitch angle and yaw angle. During ascent the second stage S30 with the payload attached achieved a maximum velocity of approx. 1950 m/s, which corresponds to a Mach number of 6.1 (Fig 10).

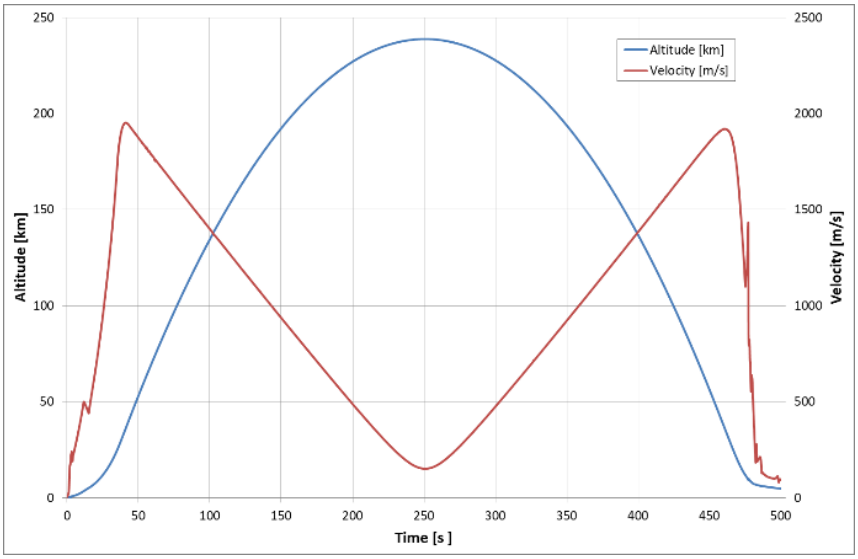

Fig 10: Altitude and velocity evolution along the flight trajectory

The unit Reynolds number at this flight point is approx. 10^6. Due to decreasing density with increasing altitude the Reynolds number decreases rapidly (Fig 11). After burn-out, the second stage S30 continued the flight on a ballistic trajectory and landed approx. 500 seconds after the take-off at a distance of approx. 67 km from the launch site. Fins of S30 did not survive its uncontrolled entry flight and were fully destroyed at flight time point of 469 seconds after lift-off. The payload has been decelerated in the late subsonic flight phase using a two-stage parachute system to avoid a hard impact and touched down on ground after approx. 800 seconds flight time. The second stage S30 experienced a hard ground impact at a speed of approx. 100 m/s after a planned uncontrolled descent flight.

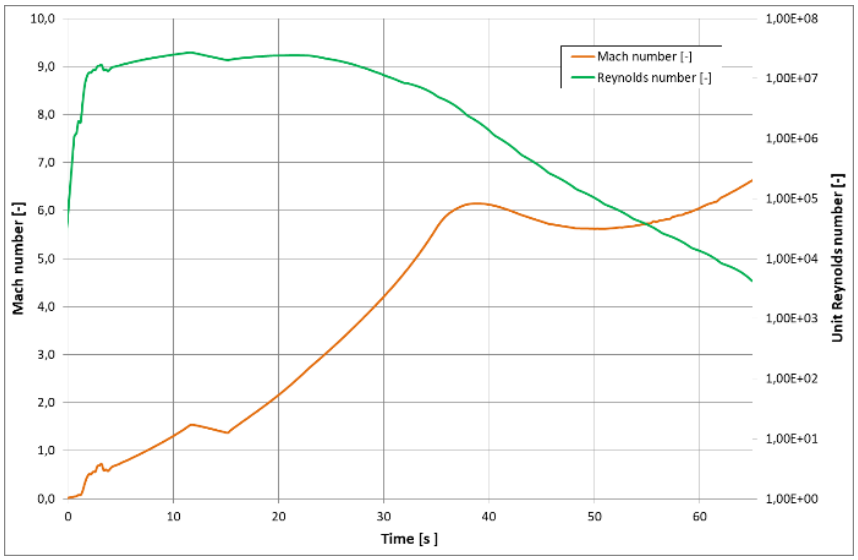

Fig 11: Mach number and Reynolds number evolution along the flight trajectory

5. Main Achievements

The Health Monitoring System allowed the measurement of aerothermal and mechanical loads on the hybrid payload structure, motor adapter, motor case, tail can and fins along the complete flight. Part of the data has been transmitted during flight to ground via telemetry at a low sampling rate of several Hertz. In addition, several impact-resistant data acquisition units could acquire the data at a high sampling rate of several Kilohertz and stored it onboard. The hybrid payload structure and health monitoring data acquisition units have been recovered after the flight and showed complete functionality. These results demonstrate flight qualification of the following payloads and technologies:

5.1. Aerodynamics and Flight Control

As mentioned before the instrumentation and further hardware accommodated in the tailcan moved the centre of gravity of the S30 stage backwards and caused reduction of the aerodynamic stability margin of this stage. Fig 10 and Fig 11 confirm that both measures like integrating a 26 kg balance mass and putting an empty segment between the motor adapter and micro-gravity experiment modules were sufficient to guarantee a successful flight concerning aerodynamic stability.

Approx. 13 seconds after lift-off, the first stage S31 of the VSB-30 launcher is burned-out and separated. Two seconds after its separation the second stage S30 was ignited and provided thrust for 29 seconds. The fins of both S31 and S30 motors were slightly inclined, in order to build up a roll rate minimizing effects on impact point dispersion during ascent. The roll frequency achieved a maximum value of approx. 2.83 Hz and pitch and yaw rates stayed at a very low level as predicted. A yo-yo de-spin system is necessary to reduce roll rate to around zero before RCS operation begins. It consists of two release mechanisms placed diametrically opposite each other on the circumference of the rocket. Steel cables, attached to hooks on the release mechanism, are wound around the body in the opposite direction to the roll sense. Weights on the end of these cables are mounted on the release mechanism. When de-spin is initiated, the released weights begin to move outwards, unwinding and slowing the angular speed of the rocket to zero. When unwinding is complete, the cables disengage from their hooks.

As shown in Fig 12 after approx. 57 seconds ascent flight a de-spin maneuver by a yo-yo system was initiated and three seconds later the S30 was separated from the payload. The roll rate sensor, which was saturated until the time point of 58.5 seconds, shows the de-spin evolution by means of yo-yo and RCS systems very clearly. As shown in the figure during this first 60 seconds an aerodynamically stable flight could be achieved. The cold gas RCS activated at T+61s allowed decreasing pitch, yaw and roll rates to approx. 0 deg/s.

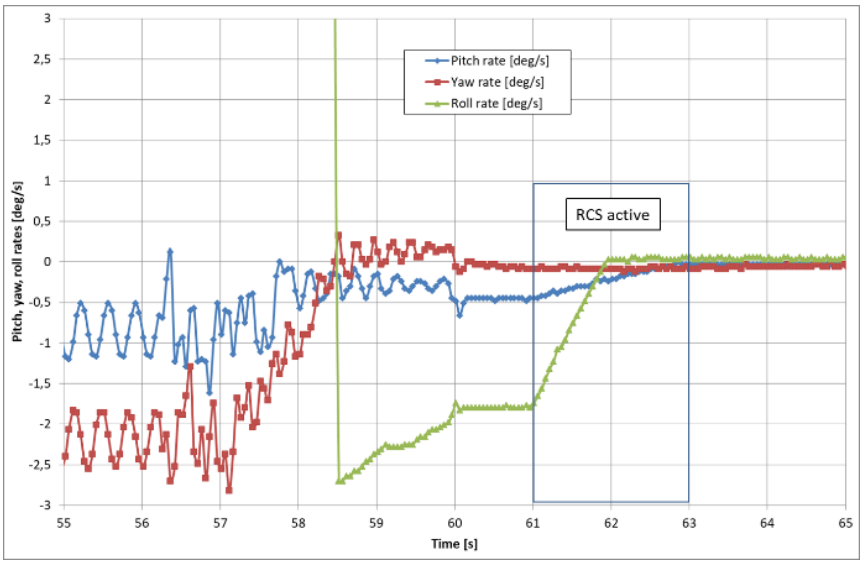

Fig 12: Pitch, yaw and roll rates evolution during ascent

5.2. Instrumented Hybrid Payload Module

Automated Fiber Placement (AFP) has been used to manufacture a sounding rocket primary structure comprised of carbon fiber-reinforced thermoplastic (CF-PEEK) [4]. Unlike many contemporary thermoplastic parts produced using AFP technology, this structure required no post-consolidation process to ensure structural integrity. This single-step (in-situ) manufacturing method has long been a target in the thermoplastic community, eliminating expensive and time-consuming vacuum-bagging processes. The manufacturing technology used to produce this component also displays a significant advantage over winding processes, where roving intersections lead to fiber undulations and hence decreased stiffness and strength. Instead, excellent geometrical tolerances and inter-ply consolidation quality were achieved, as well as superior thermomechanical properties through a tailored anisotropic laminate lay- up.

Operational loads are transferred to the structure via HI-LOK screw rivets, with qualification testing under compression, bending, and shear conditions having been successfully completed in 2018. As part of the DLR ATEK mission, this component represents the first generation of in-situ AFP-produced primary structures used in real flight applications. This module, which passed all qualification tests, successfully, represents the first generation of in-situ AFP-produced primary structures for real flight applications. The payload has been equipped with thermocouples and fiber Bragg grating (FBG) and strain gauges. The inner wall temperature distribution has been measured at a 1 kHz sampling rate using optical fibers integrated along the structure surface.

As mentioned before the hybrid module was integrated into the MAPHEUS8 scientific payload section of the ATEK flight experiment with multiple microgravity experiments. This payload section was separated from the upper stage motor S30 and made a soft landing by means of a parachute system (Fig 13, left). The right-hand side of Fig 13 shows the hybrid module coated with a heat protection cork ablator layer before and after ATEK flight experiment. Except the change of the cork layer colour, which is typical for the pyrolysis process of cork ablators in high temperature environment, no anomalies were detected

Fig 13: Microgravity experiment section MAPHEUS 8 with integrated hybrid module after ground impact (left) and Hybrid module before and after (right) the flight

The Health Monitoring System (HMS) of the hybrid module consists of type K thermocouples, strain gauges and FOS-FBG (temperature) sensors [5]. The temperature profile shows the main heating during atmospheric ascend and decent phases (Fig 14:). Compared to the uncontrolled return flight of the second stage with high speed ground impact, the hybrid module had a controlled descent and soft landing with deployed parachute. Therefore, the flight time of events is different than the second stage descent flight. Thermocouples HY2_TC01 and HY2_TC04 under the cork layer of the hybrid module measured almost the same surface temperature evolution with a slight discrepancy in the flight time period between 60 second and 80 seconds. Differences in the integration of these type K thermocouples in particular the contact interface to the module including high temperature adhesive might be the main driver of this difference.

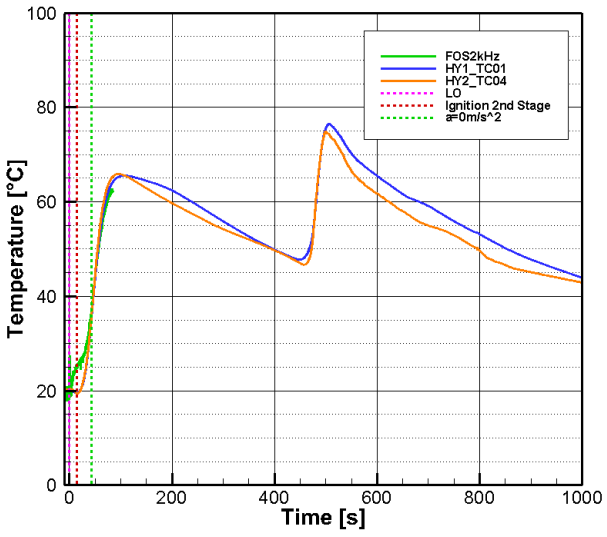

Fig 14: Measured temperature evolution at the hybrid module wall along the complete ascent and descent flight

5.3. Health Monitoring for the Motor Adapter, Motor Case, Tailcan and Fins

The motor adapter was coated with a cork based thermal protection layer. Thermocouples measure the structure temperature below the cork [5]. Two instrumented cork free metallic stripes with a width of 25mm and 50mm allowed to measure the temperature evolution of the segment and the thermal efficiency of the cork layer. A recently developed in-house heat flux sensor has measured the total heat flux evolution at selected positions. This data in combination with several thermocouples, which recorded the structure temperature, have been used for the validation of aerothermal design tools. The data acquisition has been performed using a modular and impact-resistant system.

The tailcan Health Monitoring package detects thermo-structural properties of the motor case, nozzle, fins and the tailcan with different types of instrumentation. The motor case temperature has been measured with fiber Bragg gratings. One fin has been instrumented with strain gauges, thermocouples and pressure sensors. Fin surface temperature distributions have been monitored using a compact infrared camera installed in the tailcan. In addition, an infrared camera has been placed inside the tailcan to monitor the external wall temperature of the nozzle throat region. A multiband radiometer system allowed measuring the radiative heating in the base area of the second stage motor S30.

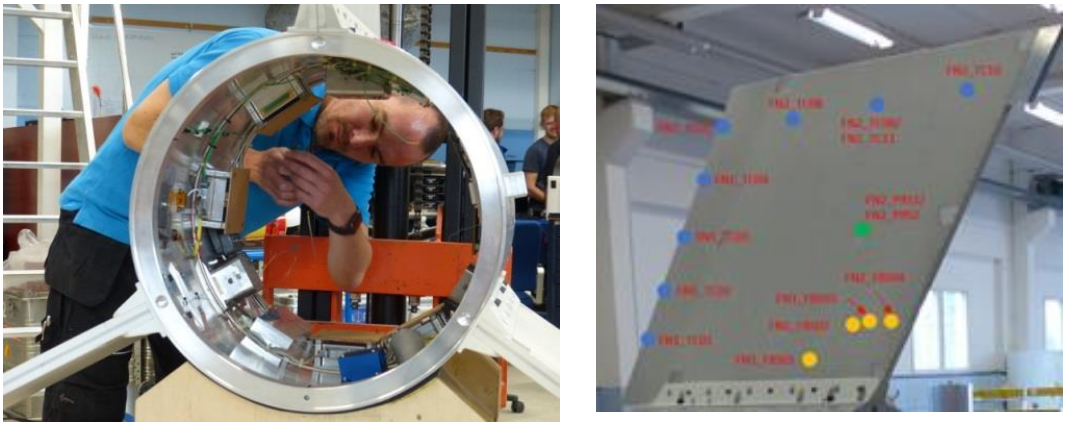

Fig 15: Tailcan instrumentation (left) and fin instrumentation (right)

Special attention has been paid to the fin instrumentation, since fins are essential for the aerodynamics of the flight vehicle and are exposed to high aerothermal loads. Therefore, one of the fins was equipped with 2 pressure transducers, 5 strain gauges, 2 radiometers and 13 thermocouples [5]. Thermocouples are divided in two groups. The first group measures the temperature of the leading-edge made of stainless steel. FN1_TC01, FN1_TC2 and FN1_TC04 have a distance of 140mm, 280mm and 560mm from origin bottom left, respectively (Fig 15). Second group thermocouples measure the structure temperature at the inner wall of fin skin, FN2_TC08…FN2_TC11 with distance horizontal from top right 500mm, 315mm and 130mm distance to top edge is 50mm.

The temperatures measured with thermocouples TC02, TC03 and TC04, which are positioned in the middle section of the fin leading edge, follow similar evolution over the complete ascent and flight time (Fig 15). The maximum fin leading edge temperature is achieved at the flight time point of 44 seconds and is near to the material operating temperature. Due to the deceleration of the vehicle due to gravitational forces and slight atmospheric drag in the flight phase without thrust aerothermal decreases and leads to decreasing temperatures.

Approx. 75 seconds after the lift-off the second stage with payloads has an altitude of 100 km and is not exposed to atmospheric effects any more. The further decrease of the temperature is caused by radiative cooling of the fin structure. The temperature of the thermocouple TC05 has a lower peak value during ascent and remains below temperatures of other thermocouples along the complete flight phases. An imperfect contact of the thermocouple TC05 to the structure may be responsible for this behaviour. TC05 data shows a delayed response to aerothermal heating. A similar tendency is observed

in the response of TC01, which is mounted to the interface between the fin and tailcan. The radial distance from the interface line is 120 mm. It is possible that this sensor was exposed to the boundary layer flow or separated flow.

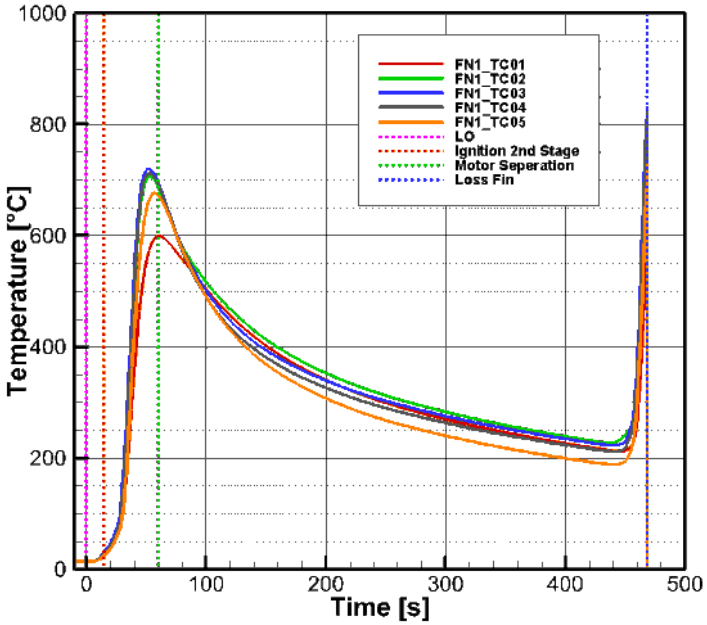

Fig 16: Measured temperature of the fin leading edge structure

5.4. Impact-resistant Data Acquisition System

The payload data acquisition system for Health Monitoring has been modularly designed [6]. This feature allows short harnesses for widely distributed sensors and simplifies the integration of the components in particular for spacecrafts with limited volume available. Different types of sensors can be connected to the acquisition unit. Each measurement channel can be configured individually to use the complete dynamic range of the sensors. The acquired data can be transmitted to the ground station via telemetry or stored in the impact-resistant storage unit. Due to its own battery the data acquisition is autonomous. Using additional modules further payloads like infrared cameras, FOS units, etc. can be connected.

As mentioned before the second stage booster S30 experienced a planned uncontrolled re-entry flight, which ended at a high-speed impact on ground. The condition of the stage after high speed impact is shown in Fig 17. The motor adapter and tailcan/fin components are destroyed. But, all data acquisition elements units and memory units could be recovered after hard ground impact of the second stage at an impact velocity of around 100 m/s. The damages to the cases of data acquisition boxes after the ground impact are visible (Fig 18). But, all impact-resistant storage units (lower line) survived the impact and showed full functionality. The analysis of data after downloading it from memory units confirmed a completely working system worked form lift-off until ground impact.

Fig 17: Second stage (S30 motor) after ground impact

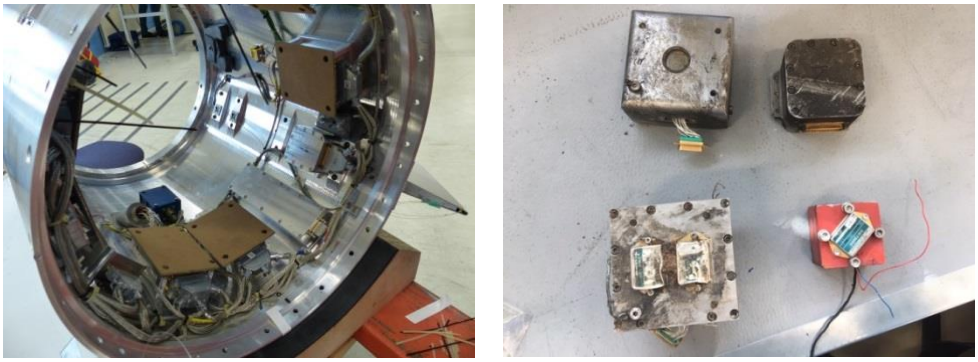

Fig 18: Impact-Resistant Data Acquisition System before (left) and after (right) the flight.

6. Concluding remarks

The sounding rocket flight experiment ATEK with several scientific payloads has been carried out successfully and provided valuable flight data. The second stage S30 of the flight configuration and the payload reached an apogee of approx. 240 km. The second stage continued the descent on a ballistic trajectory and landed approx. 500 seconds after the take-off at a distance of approx. 67 km from the launch site. The payload was decelerated in the late subsonic flight phase using a two-stage parachute system to avoid a hard impact on ground and touched down after approx. 800 seconds flight time. The Health Monitoring System allowed to measure aerothermal and mechanical loads on the hybrid payload structure, motor adapter, motor case, tailcan and fins along the complete flight. Part of the data has been transmitted during flight to ground via telemetry at a low sampling rate of several Hertz. In addition, several impact-resistant data acquisition units acquired data at a high sampling rate up to one Kilohertz and stored it onboard. The hybrid payload structure and health monitoring data storage units have been recovered after the flight and showed complete functionality. The expertise gained during ATEK activities allowed us to perform the unique hypersonic flight experiment with significantly higher aerothermal loads achieved using a three stages sound rocket configuration [7].

7. Acknowledgment

The research project ATEK including the flight experiment was fully funded by the DLR's Program Directorate for Space Research and Development.

References

1. Ali Gülhan, Dominik Neeb, Thomas Thiele and Frank Siebe; Aerothermal Postflight Analysis of the Sharp Edge Flight Experiment-II. Journal of Spacecraft and Rockets, DOI: 10.2514/1.A33275. ISSN 0022-4650.
2. Thiele, T., Neeb, D., and Gülhan, A., "Post-Flight Hypersonic Ground Experiments and FADS Flight Data Evaluation for the SHEFEX-II Configuration," Proceedings of 8th European Symposium on Aerothermodynamics for Space Vehicles, ESA, March 2015.
3. T. Thiele, A. Gülhan, H. Olivier; Instrumentation and Aerothermal Postflight Analysis of the Rocket Technology Flight Experiment ROTEX-T, Journal of Spacecraft and Rockets, Vol. 55, No. 5, September–October 2018.
4. A. Chadwick, P. Dreher, I. Petkov, S. Nowotny: A. Fibre-reinforced Thermoplastic Primary Structure for Sounding Rocket Applications, SAMPE Europe, Nantes, France, 2019.
5. F. Klingenberg, F. Siebe, A. Gülhan; Instrumentation of ATEK Flight Experiment, HiSST: 2nd International Conference on High-Speed Vehicle Science Technology, 11-15 September 2022, Bruges, Belgium.

6. F. Siebe, F. Klingenberg, R. Kronen, A. Gülhan; Autonomous Data Acquisition System for the Hybrid-Structure and the 2nd Stage of the Sounding Rocket flight Experiment ATEK, HiSST: 2nd International Conference on High-Speed Vehicle Science Technology, 11-15 September 2022, Bruges, Belgium.
7. A. Gülhan, D. Hargarten, F. Klingenberg, F. Siebe, G. di Martino, T. Reimer; Main Results of the Hypersonic Flight Experiment STORT, HiSST: 2nd International Conference on High-Speed Vehicle Science Technology, 11-15 September 2022, Bruges, Belgium.